Configuration Optimization of Anchoring Devices of Frame-Supported Membrane Structures for Maximum Clamping Force

Taku Nakajima [1], Makoto Ohsaki [2], Jun Fujiwara [3] and Fumiyoshi Takeda [3]

[1]Dept. of Architecture and Architectural Engineering, Kyoto University, Kyoto 615-8540, Japan
rp2-nakajima@archi.kyoto-u.ac.jp
[2]Dept. of Architecture, Hiroshima University, Higashi-Hiroshima 739-8527, Japan
ohsaki@hiroshima-u.ac.jp
[3]Technical Research Center, Taiyo Kogyo Corporation, Hirakata 573-1132, Japan
{fj003177, tf001163}@mb.taiyokogyo.co.jp

Abstract
A method is presented for shape optimization of anchoring devices for membrane structures. The device is modeled using frame elements, and an extended ground structure approach is used for optimizing the configuration of the frame model; i.e., the cross-sectional areas, topology, and geometry (nodal locations) are simultaneously optimized. The objective function is the total structural volume, and an lower-bound constraint is given for the reaction force related to the clamping force against the membrane under the external load representing the membrane tensile force. We also present an optimization result of a frame model that enables us to adjust deformation of membrane by applying a clamping force with a bolt against the anchoring device. Finally, we present another model of the anchoring device that can be stabilized by buckling and contact by considering material and geometrical nonlinearity.

Keywords: *Membrane structure, Anchoring device, Configuration optimization, Stress constraints*

1. Introduction

Recent rapid development of computational technology enabled us to optimize shapes and topologies of large-scale structures considering realistic and complex responses such as inelastic and dynamic responses. There have been many practical applications for optimization of mechanical parts. The second author presented a method of optimizing shapes of beam flanges for maximizing the plastic energy dissipation under cyclic deformation [1, 2]. Therefore, it is possible to optimize performances of mass-produced structural parts also in the field of civil and architectural engineering.

Membrane structures are widely used for covering large space with lightweight membrane material. Fig. 1 illustrates an anchoring device of a membrane structure. Membrane structures are generally connected to the boundary frames with anchoring devices, which are made of aluminum alloy by extrusion molding. Since such devices are mass-products and have large portion of the total weight of the membrane structure, it is possible that the total production cost can be reduced by optimizing shapes and cross-sectional properties of the devices. Furthermore, when external loads such as wind loads are applied to the membrane, its tensile forces increases and anchoring devices are subjected to large deformation, which may cause detachment of the membrane from the device before the fracture of membrane material. Therefore, the load resistance capacity of the membrane structure can be improved by optimizing the anchoring devices so that the clamping force is increased as a result of the increase of tensile force of the membrane.

In this study, we present a method for optimizing anchoring devices modeled by frame elements. An extended ground structure approach is used for optimizing the configuration of the frame model; i.e., the cross-sectional areas, topology, and geometry (nodal locations) are simultaneously optimized. First, the topology of the frame model is optimized for fixed nodal locations. The objective function is the total structural volume, which is to be minimized, and the constraint is given for the clamping force against the membrane. The external load representing the membrane tensile force is applied, and the assumption of small deformation is used. We also present an optimization result of a frame model that enables us to adjust deformation of membrane by applying a clamping force with a bolt against the anchoring device. Finally, we present another model of the anchoring device that can be stabilized by buckling and contact by considering material and geometrical nonlinearity, which is an extension of the compliant mechanism presented by the second author [3]. For this purpose, the general purpose finite element solver called ABAQUS is successfully combined with a nonlinear programming library using a script language called Python. This way, the deformed shape can be retained without bolts reinforcing and sufficient tensile force is ensured for the membrane.

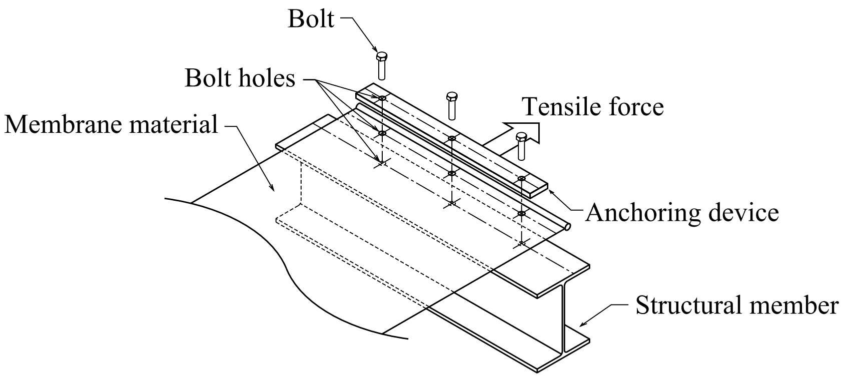

Figure 1. Overview of an anchoring device.

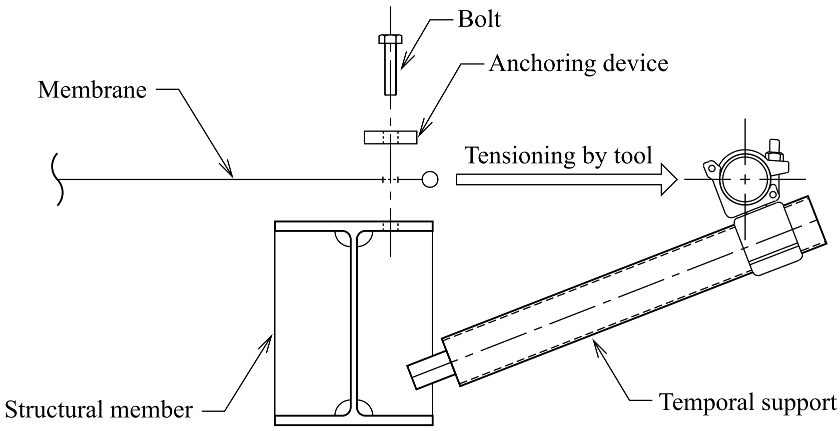

Figure 2. Constraction process.

2. Overview of tensioning process of and anchoring device of membrane structure.
Construction process of membrane strucutres are outlined in Fig. 2 In this process, temporal supports are first fitted to the structural members. Obtaining reaction force from the supports, the membrane is pulled (tensioned) by tool until the preassigned holes of the membrane and are located on the bolt holes of the structural member. Finally, the membrane is pressed to the frame using tha anchoring device and bolts. However, in this process, there exist the following difficulties:

1. Adjustment of tensile force is very difficult because the holes are assigned at predetermined locations.
2. Temporal supports for obtaining reaction force and tensioning tools are needed in addition to the structural members.

In the following, optimization approaches are presented for overcoming these difficulties. The device is modeled as a frame consisting of beam rigidly connected elements, and an extended ground structure approach is used for optimizing the confiuguration (topology and nodal locations) of the frame.

3. Frame model (Type 1)
We first find the overall configuration of the device that automatically clamps the membrane as the result of introducing tensile forces to the membrane. The device is modeled as a frame with small elastic deformation.

Consider a frame (Type 1) as shown in Fig. 3 as the ground structure for finding the optimal topology, where the intersecting diagonal members are rigidly connected at the centers. The frame is supported with roller at support 1 and fixed at supports 2 and 3. The member is supposed to have solid rectangular section with the fixed width b. A load P is applied in the negative x-direction at node 1. The total structural volume V is minimized under constraints such that the vertical reaction R_1 at node 1 is greater than the specified value $\overline{R}$.

The design variables are cross-sectional areas $\boldsymbol{A} = (A_1, \dots, A_m)^\top$ of the members, where m is the number of members. The upper and lower bounds of A_i is denoted by A_i^{U} and A_i^{L}, respectively. A constraint is given for the maximum absolute value $|\sigma_i|$ of the stress of the ith members is less than the specified upper bound $\bar{\sigma}$. Then the optimization problem is

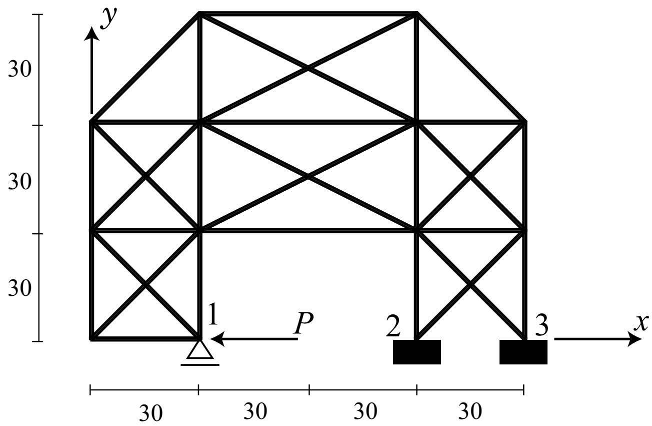

Figure 3. Frame model (Type 1)

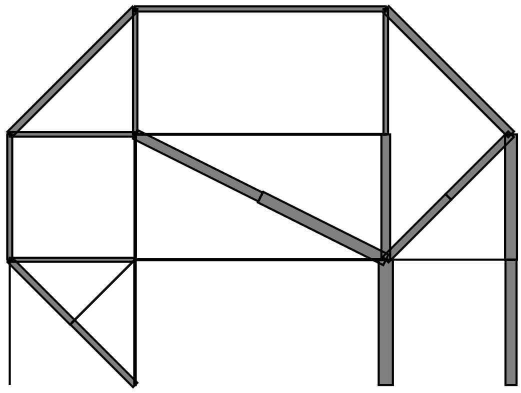

Figure 4. Optimal configuration with stress constraints.

formulated as

$$\begin{aligned} &\text{minimize} && V(\boldsymbol{A}) && \text{(1a)}\\ &\text{subject to} && |\sigma_i| \leq \bar{\sigma} \qquad (i = 1, ..., m) && \text{(1b)}\\ &&& R_1 \geq \bar{R} && \text{(1c)}\\ &&& \boldsymbol{A}^{\mathrm{L}} \leq \boldsymbol{A} \leq \boldsymbol{A}^{\mathrm{U}} && \text{(1d)} \end{aligned}$$

Optimization is carried out using the software library SNOPT Ver. 7.2 [5] utilizing sequential quadratic programming. The sensitivity coefficients are computed with finite difference approach. The elastic modulus of the members is 2.0×10^5 N/mm^2, and the width of each member is 10 mm. A load $P = 500$ N is applied in the negative x-direction at node 1. The lower bound $\bar{R}$ for reaction is 200 N. The cross-sectional areas of all the 42 members are independent variables with lower bound $A_i^{\mathrm{L}} = 0.1$ mm^2, whereas different values of A_i^{U} are used for the optimization problems below. The upper bound stress is $\bar{\sigma} = 200$ N/mm^2. In the following, the units of length and force are mm and N if not explicitly specified. A uniform random number $r_i \in [0, 1)$ is generated to obtain the initial value of A_i as $50r_i + 1.0$. The best solution from ten different initial solutions is taken as the optimal solution.

Optimization is carried out for the upper-bound cross-sectional area $A_i^{\mathrm{U}} = 200$. The optimization result after removing the members with $A_i = A_i^{\mathrm{L}}$ is as shown in Fig. 4, where the height of each member is drawn with real scale. Note that the reaction constraint is active as $R_1 = \bar{R} = 200.0$, and the objective function value is $V = 1.1018 \times 10^4$. The reaction constraint is active for all optimal solutions below.

If all cross-sectional areas have the same value 10, then $R_1 = -137.71$; therefore, the direction of reaction has been successfully reversed through optimization. As is seen from Fig. 4, the number of members is not drastically reduced, because stress constraints should be satisfied in all members including very thin members. It is well known in truss topology optimization that the number of members cannot be successfully reduced by conventional ground structure

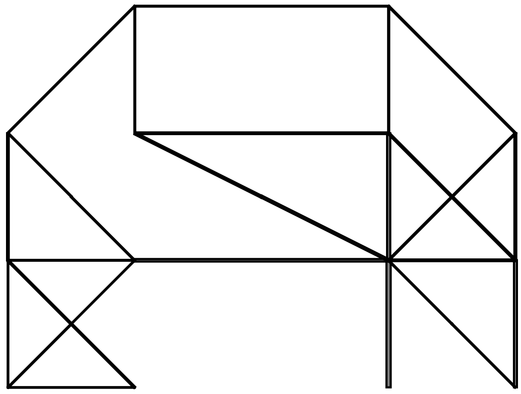

Figure 5. Optimal topology for $\bar{U} = -0.1$.

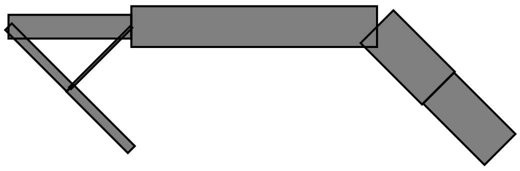

Figure 6. Optimal topology for $\bar{U} = -0.01$.

Figure 7. Optimal topology for $\bar{U} = -0.1$ with stiffness penalization $p = 6$.

approach with nonlinear programming [7, 8]. Therefore, we next carry out optimization with displacement constraint and without stress constraints as follows:

$$\begin{aligned}
&\text{minimize} && V(\boldsymbol{A}) && \text{(2a)}\\
&\text{subject to} && U_1 \geq \bar{U} && \text{(2b)}\\
& && R_1 \geq \bar{R} && \text{(2c)}\\
& && \boldsymbol{A}^{\mathrm{L}} \leq \boldsymbol{A} \leq \boldsymbol{A}^{\mathrm{U}} && \text{(2d)}
\end{aligned}$$

where $\bar{U}$ is the lower bound for the x-directional displacement U_1 (< 0) of support 1.

Optimal configuration is found for $\bar{U} = -0.1$ and $A^{\mathrm{U}} = 1000$. The best solution among those from ten different initial solutions is taken also for this case. The optimal topology is as shown in Fig. 5, where the height of each member is scaled by 1/5. The optimal objective value is $V = 1.6781 \times 10^4$.

The optimal solution for $\bar{U} = -0.01$ is as shown in Fig. 6 with $V = 6.7593 \times 10^4$. Therefore, the number of members decreases and the heights of existing members increase as the displacement constraint becomes tight. However, the maximum height is 56.439, which is unrealistic. Hence, the displacement bound is conceived as an artificial parameter for controlling the number of members in optimal topology.

The stiffness of a thin member can be penalized in the similar manner as SIMP method for continuum topology optimization. For the solid rectangular section with the height h, the bending stiffness is proportional to h^p with $p = 3$. However, if we increase p artificially to 6, we obtain the optimal solution as shown in Fig. 7 that has few members. Therefore, increasing p is equivalent to decreasing the absolute value of displacement bound.

We next solve the optimization problem with stress constraint for the optimal topology in Fig. 6. Note that displacement constraint is not assigned. The optimal solution is as shown in Fig. 8 with real scale, where $V = 1.8748 \times 10^4$.

The optimal solution is discretized to shorter members, and optimization is carried out again with y-coordinates of nodes as design variables. Let Y_i denote the initial y-coordinate of the ith node. Then the lower and upper bounds for Y_i

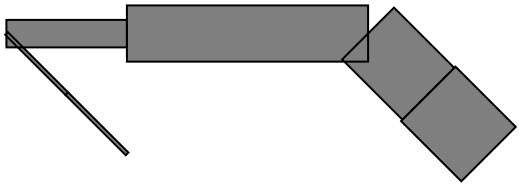

Figure 8. Optimal solution under stress constraints.

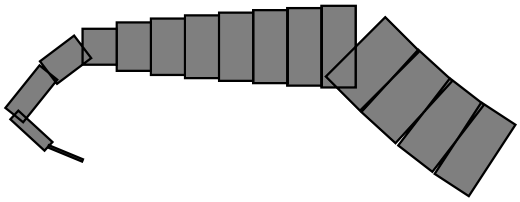

Figure 9. Optimal solution under stress constraints with variable nodal locations.

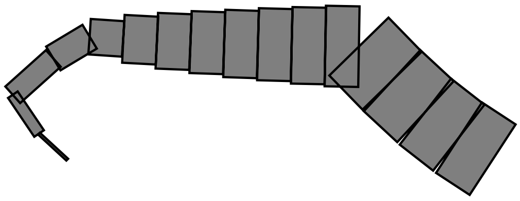

Figure 10. Deformed shape of optimal solution under stress constraints with variable nodal locations.

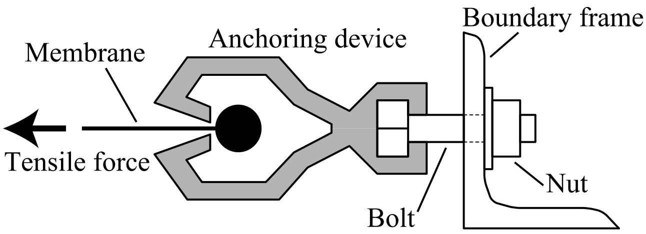

Figure 11. Illustration of anchoring device (Type 1)

are given as $Y_i - 5$ and $Y_i + 20$, respectively. The optimal shape is as shown in Fig. 9 with $V = 1.7082 \times 10^4$. Fig. 10 shows the deformed shape with magnification factor 20.

4. Frame model (Type 2)

It has been demonstrated in the previous section that a shape that has increasing clamping force with increasing tensile force can be found by optimization of cross-sectional areas, topology, and nodal locations of a frame model. From this result, we can construct an anchoring device as shown in Fig. 11. However, the tensile force cannot be adjusted by pulling the membrane using this device. Therefore, in the following, optimization is carried out for another frame model (Type 2) as shown in Fig. 12 with vertical force representing the compression force of a bolt. The frame is an simplification of the device as shown in Fig. 13. The loads P_1 and P_2 represent the forces from membrane and bolt, respectively.

The load $P_2 = 300$ is first applied in the vertical direction at node 2. Then the y-directional displacement is fixed at node 2, and the load $P_1 = 500$ is applied in the horizontal direction at node 1. Initial solutions are generated in the same manner as the previous example.

Let $U_1^{(1)}$ denote the displacement of node 1 against P_1. The displacement of node 1 after application of P_1 and P_2 is

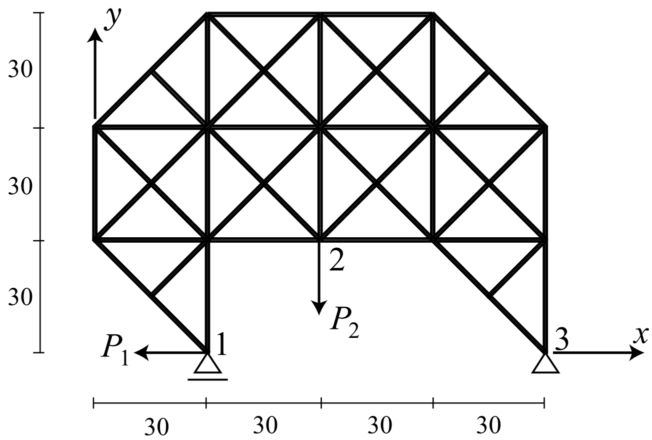

Figure 12. Frame model (Type 2)

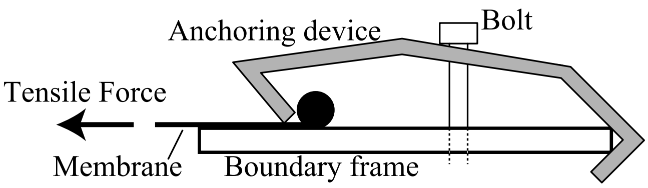

Figure 13. Illustration of anchoring device (Type 2)

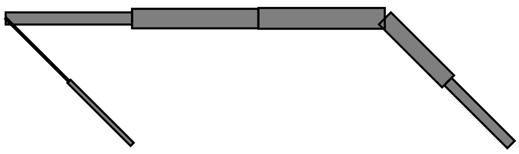

Figure 14. Optimal solution of Type 2 under displacement constraint.

denoted by $U_1^{(2)}$. Then the optimization problem is stated as

$$\begin{aligned} &\text{minimize} && V(\boldsymbol{A}) && \text{(3a)} \\ &\text{subject to} && U_1^{(1)} \geq \bar{U}^{(1)} && \text{(3b)} \\ & && U_1^{(2)} \geq \bar{U}^{(2)} && \text{(3c)} \\ & && \boldsymbol{A}^{\mathrm{L}} \leq \boldsymbol{A} \leq \boldsymbol{A}^{\mathrm{U}} && \text{(3d)} \end{aligned}$$

Note that $U_1^{(1)} \leq 0$ and $U_1^{(2)} \geq 0$.

The optimal solution scaled by 1/10 for $\bar{U}^{(1)} = -0.01$ and $\bar{U}^{(2)} = 0.1$ is shown in Fig. 14, which has sufficiently small number of members. Optimization is carried out under stress constraints after subdivision of members. The y-coordinates of nodes are also design variables. The problem is stated as

$$\begin{aligned} &\text{minimize} && V(\boldsymbol{A}) && && \text{(4a)} \\ &\text{subject to} && U_1^{(1)} \geq \bar{U}^{(1)} && && \text{(4b)} \\ & && U_1^{(2)} \geq \bar{U}^{(2)} && && \text{(4c)} \\ & && |\sigma_i^{(1)}| \leq \bar{\sigma} && (i = 1, ..., m) && \text{(4d)} \\ & && |\sigma_i^{(2)}| \leq \bar{\sigma} && (i = 1, ..., m) && \text{(4e)} \\ & && \boldsymbol{A}^{\mathrm{L}} \leq \boldsymbol{A} \leq \boldsymbol{A}^{\mathrm{U}} && && \text{(4f)} \end{aligned}$$

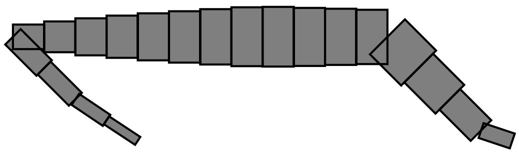

Figure 15. Optimal solution of Type 2 under stress constraints.

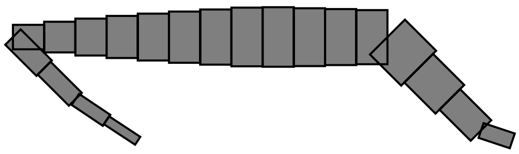

Figure 16. Optimal solution of Type 2 under stress constraints; deformation magnified by 20 after application of P_2.

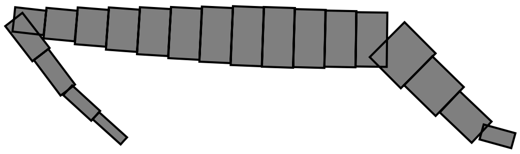

Figure 17. Optimal solution of Type 2 under stress constraints; deformation magnified by 20 after application of P_1 and P_2.

where $\sigma_i^{(1)}$ and $\sigma_i^{(2)}$ are the stresses of member i against P_1 and P_2, respectively. The optimal solution is shown in Fig. 15 with real scale. The deformed shapes against P_2 as well as the shape after application of P_1 and are shown in Fig. 16 and Fig. 17.

5. Shape optimization utilizing snapthrough.

In the previous examples, we optimized frame models with assumption of small deformation. In this section, optimal shape is found considering material and geometrical nonlinearities to obtain a device that can be stabilized after deformation utilizing snapthrough and contact.

Consider a frame model (Type 3) as shown in Fig. 18, where the horizontal coordinates of nodes 1, 2, and 3 are 0, 30, and 80, respectively. All members consist of beam element except member 6, which is a truss element with cross-sectional area 20. The width is 10 for all beams. The heights of beams are 2 except 1 for member 1. The material is alminuum with elastic modulus 7.0×10^4, Poisson's ratio 0.3 and yield stress 200. The linear kinematic hardening with ratio 1/100 is used for beams, whereas the truss is assumed to be elastic.

The design variable vector $\boldsymbol{X}$ includes the y-coordinates of all the nodes except supports. Let X_i^0 denote the value of the ith variable in Fig. 18. Then the bounds for X_i are given by $X_i^0 - 5.0$ and $X_i^0 + 5.0$. Forced displacement is given at node 2 in the vertical direction until the final state when a member contacts node 3. The objective function is the reaction R_4 at node 4 that is to be minimized. A constraint is given for the x-directional displacemnet u_2 of node 2 at the final state as $u_2 \leq 1$. Then the optimization problem is formulated as

$$\begin{aligned} \text{minimize} \quad & F(\boldsymbol{X}) = -R_4 \\ \text{subject to} \quad & u_2 \geq 1.0 \\ & \boldsymbol{X}^{\mathrm{L}} \leq \boldsymbol{X} \leq \boldsymbol{X}^{\mathrm{U}} \end{aligned} \tag{5}$$

A finite element analysis software package ABAQUS Ver. 6.5 [6] is used for analysis. The frame is modeled by element beam B21 considering shear deformation, and analysis is carried out by arc-length method. The script language Python is used for the interface between ABAQUS and optimization package SNOPT.

The optimal shape and its deformed state are shown in Fig. 19. The load-displacement relation at node 4 is plotted in Fig. 20. The vertical reaction at node 4 at the final state is −11.15 for the initial solution and −2.627 for the optimal solution. The horizontal displacement u_2 is −2.11 mm, which does not satisfy the constraint, for the initial solution, and 1.00 mm for the optimal solution. Since the frame is stable owing to the contact between support 3 and members 4 and 5 , the final state is retained without bolt and the tensile force of membrane is maintained. Furthermore, the tensile force

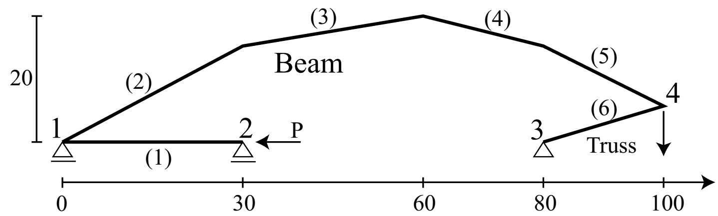

Figure 18. Frame model (Type 3)

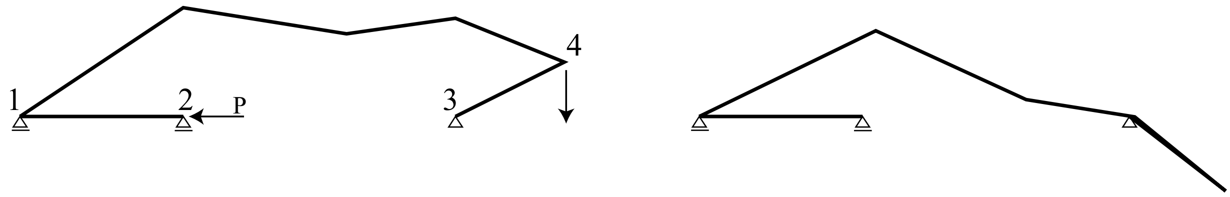

Figure 19. Optimal shape and its deformed state

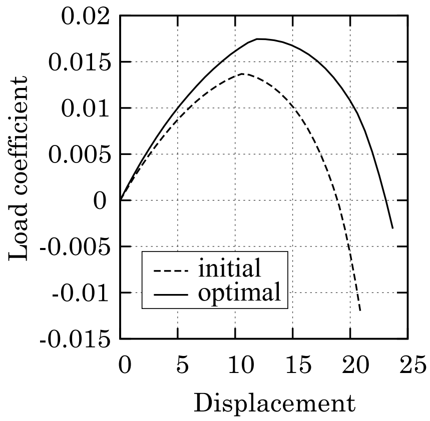

Figure 20. Load-displacement relation at node 4.

can be adjusted through modification of displacement of node 4.

6. Conclusion

Shape and topology optimization has been carried out for anchoring device of membrane structures modeled by beam elements. The total structural volume is minimized under constraint on the reaction so that the clamping force increases as the result of increasing membrane tensile force.

It has been shown that an optimal topology has many members if stress constraints are assigned for all members. This result is similar to the truss topology optimization under stress constraints. Therefore, an optimal topology with small number of members is obtained by relaxing the stress constraints and assigning displacement constraint.

Optimal solution with few members can be found if very strict bound for the displacement and very large upper bounds for cross-sectional areas are given, because the bending stiffness is proportional to the cubic power of the height and a member with larger height is more efficient than that with smaller height. The stiffness of a member with small height can also be penalized using the approach similar to the SIMP method for continuum topology optimization.

The optimal topology can be further optimized with subdivided members and stress constraints, where the vertical coordinates of nodes are also considered as design variables.

A shape of the device that pulls the membrane efficiently by applying vertical force through a bolt can also be found by optimization. Finally, a device that clamps the membrane without external load has been optimized utilizing snapthrough and contant.

Acknowledgement
Financial support by Nohmura Foundation for Membrane Structure's Technology is gratefully acknowledged.

References

1. P. Pan, M. Ohsaki and H. Tagawa, Shape optimization of H-beam flange for maximum plastic energy dissipation, J. Struct. Eng., ASCE, Vol. 133(8), pp. 1176–1179, 2007.

2. M. Ohsaki, H. Tagawa and P. Pan, Shape optimization of reduced beam section for maximum plastic energy dissipation under cyclic loads, J. Constructional Steel Research, Vol. 65, pp.1511–1519, 2009.

3. M. Ohsaki and S. Nishiwaki, Shape design of pin-jointed multistable compliant mechanism using snapthrough behavior, Struct. Multidisc. Optim., Vol. 30, pp. 327–334, 2005.

4. H. Kim, M. Kawabata, Study on stress transition mechanism of clamping part of membrane structures – tensile and fracture characteristic of membrane material in bolting part –, Research Report on Membrane Structures 2005, No. 19, pp.41–48, 2005 (Japanese).

5. P. E. Gill, W. Murray and M. A. Saunders, SNOPT, An SQP algorithm for large-scale constrained optimization, SIAM J. Optim., Vol. 12, pp. 979–1006, 2002.

6. ABAQUS Ver. 6.5 Documentation, ABAQUS Inc., 2005.

7. G. Cheng and X. Guo, ε-relaxed approach in structural topology optimization, Struct. Opt., Vol. 13, pp. 258–266, 1997.

8. M. Ohsaki and N. Katoh, Topology optimization of trusses with stress and local constraints on nodal stability and member intersection, Struct. Multidisc. Optim., Vol. 29, pp. 190–197, 2005.